The Astrophysical Journal, 619:L183–L186, 2005 February 1

OBSERVATION OF *R*-BAND VARIABILITY OF L DWARFS

M. Maiti, S. Sengupta, P. S. Parihar, and G. C. Anupama
Indian Institute of Astrophysics, Koramangala, Bangalore 560 034, India; mith@iiap.ernet.in
Received 2004 September 9; accepted 2004 December 15; published 2005 January 6

ABSTRACT

We report, for the first time, photometric variability of L dwarfs in the *R* band. Out of three L1 dwarfs (2MASS 1300+19, 2MASS 1439+19, and 2MASS 1658+70) observed, we have detected *R*-band variability in 2MASS 1300+19 and 2MASS 1439+19. The objects exhibit variability of amplitude ranging from 0.01 to 0.02 mag. Object 2MASS 1658+70 turns out to be nonvariable in both the *R* and *I* bands. However, more observations are needed to infer its variability. No periodic behavior in the variability is found from the two L1 dwarfs that are variable. All three L1 dwarfs have either negligible or no Hα activity. In the absence of any direct evidence for the presence of a sufficiently strong magnetic field, the detection of polarization at the optical favors the presence of dust in the atmosphere of L dwarfs. We suggest that the observed *R*-band photometric variability is most likely due to atmospheric dust activity.

Subject headings: stars: atmospheres — stars: low-mass, brown dwarfs

1. INTRODUCTION

L dwarfs are ultracool objects with effective temperatures ranging between 2200 and 1400 K. They are characterized by the presence of condensates in their atmosphere. As a result of incomplete gravitational settling, dust in the atmosphere of L dwarfs could be detectable in the optical. Dust clouds can play a potential role in making the object variable. Time-resolved photometric variability of a large number of L dwarfs has been reported by Bailer-Jones & Mundt (2001a, 2001b), Martín et al. (2001), Gelino et al. (2002), Clarke et al. (2002a), Zapatero Osorio et al. (2003), and Bailer-Jones & Lamm (2003). However, all these observations were made in the *I* and *J* bands. Clarke et al. (2002b) reported variability from ultracool dwarfs by using a nonstandard filter with the effective wavelength similar to that of the *I* band. Enoch et al. (2003) reported evidence of variability in the K_s band from a few L and T dwarfs. These investigations provide much insight on the atmospheric activities, especially the presence of dust clouds.

Sengupta & Krishan (2001) argued that the presence of dust could give rise to a detectable amount of linear polarization in the optical from L dwarfs. This was observationally verified by Menard et al. (2002), who detected nonzero linear polarization at red (0.768 μm) from a few L dwarfs. In the absence of any direct evidence of a sufficiently strong magnetic field, observation of linear polarization strongly favors the presence of dust in the atmosphere of L dwarfs, and a single dust scattering model could explain the observed polarization (Sengupta 2003). It should also be mentioned here that rigorous theoretical analysis (see Burrows et al. 2001 and references therein; Tsuji et al. 2004) of the continuum spectra implies the presence of dust in the visible region of L dwarfs.

Detection of nonzero polarization at the optical band that may arise from dust scattering urges the investigation of *R*-band variability by dust activity in L dwarfs. In the present Letter, we, for the first time, report differential photometric variability in the *R* band from a few L dwarfs. The results could be a good complement to the polarization observations, as dust clouds play a crucial role in both cases. A detailed theoretical investigation on polarization by a single dust scattering of L dwarfs with fixed rotational velocity (Sengupta & Kwok 2004) shows that the degree of linear polarization peaks at L1 spectral type. This motivates us to concentrate on the observation of L1 dwarfs. We have detected photometric variability from two L1 dwarfs. In § 2, we describe the observation and data reduction procedure followed. The results are presented and discussed in § 3 and are followed by conclusions (§ 4).

2. OBSERVATION AND DATA REDUCTION

The photometric observations of selected L dwarfs were carried out during 2004 January–June using the 2 m Himalayan Chandra Telescope of the Indian Astronomical Observatory (IAO) at Hanle, India, using the Himalaya Faint Object Spectrograph Camera, equipped with a SITe 2 × 4 K pixel CCD. The central 2 × 2 K region used for imaging corresponds to a field of view of $10' \times 10'$ at $0\farcs296$ pixel^{-1}.[1]

We selected the targets from published spectroscopically determined L dwarfs, specifically selecting those objects that have negligible or no Hα effective line width. This avoids the contribution of Hα line variability to the atmospheric variability in the *R* band, and hence any variability observed could be attributed more convincingly to the presence of dust clouds. Table 1 presents the name, position, and the *R* and *I* magnitudes of those objects.

Several exposures with times of 10 and 5 minutes were obtained in the *R* and *I* bands, respectively. The central wavelengths of the *R*-band filter and the *I*-band filter used are 0.6 and 0.805 μm, respectively. To minimize the effect of improper flat-fielding and any systematic error spatially associated with the chip, we tried to confine the L dwarf to a particular CCD pixel in all the frames. The observations were carried out during a dark Moon period, and uninterrupted observations of a single object were obtained over 3–7 hr during different nights. The FWHM of the stellar profile was found to be about $1\farcs5$–$1\farcs8$. The observing log is given in Table 2. The basic image processing such as bias subtraction and flat-fielding were done in the standard manner using the various tasks available within IRAF. Atmospheric extinction and transformation coefficients were obtained from observations of photometric standard stars (Landolt 1992). The *I* frames were affected by CCD fringing due to night-sky emission lines. Fringe correction was applied

---

[1] More details on the telescope and the instrument may be obtained from http://www.iiap.res.in/iao.

TABLE 1

Basic Data of Variable L1 Dwarfs

Name	R.A. (J2000.0)	Decl. (J2000.0)	*R* Magnitude	*I* Magnitude	Hα Emission
2MASS 1300+19[a] ……	13 00 42.5	+19 12 35	18.7	16.0	…
2MASS 1439+19[b] ……	14 39 28.4	+19 29 15	18.7	16.0	<0.03
2MASS 1658+70[a] ……	16 58 03.7	+70 27 01	19.2	16.6	…

Note.—Units of right ascension are hours, minutes, and seconds, and units of declination are degrees, arcminutes, and arcseconds.

[a] From Gizis et al. (2000).

[b] From Kirkpatrick et al. (1999).

to all the *I* frames using a master fringe frame created by observing several blank night-sky fields.

The stellar magnitudes at varying apertures were then obtained using the IRAF task *phot*. Since accurate sky background estimation is very crucial to faint object photometry, the sky value was iteratively estimated by examining the growth curves of isolated stars so that the growth curves were neither monotonically decreasing (underestimated sky) nor increasing (overestimated sky). Furthermore, the magnitudes of L dwarfs and faint stars were first determined at the aperture having the highest signal-to-noise ratio, and then aperture correction was made to the aperture size 4 times FWHM using the correction term obtained from bright isolated stars. The standard *R* and *I* magnitudes of L dwarfs and the field stars were determined using system transformation coefficients.

Differential photometry was performed following the ensemble photometry technique (Gilliland & Brown 1988; Everett & Howell 2001). From the average flux of the few fairly bright stars, we determined the ensemble reference magnitude, iteratively rejecting stars that were found to have either a systematic variation or large errors. The differential magnitude of L dwarfs with respect to the ensemble magnitude was then computed using the relation

$$\Delta m_{i,b} = \bar{m} - m_{i,b}, \tag{1}$$

where $\bar{m}$ is the ensemble magnitude and $m_{i,b}$ is the magnitude of L dwarfs.

While analyzing the differential photometric data of L dwarfs, a linear variation with respect to air mass was noticed. This trend appears to be an effect of the second-order extinction coefficient. The spectral type of the observed ultracool dwarfs was L1, whereas our ensemble references were found to be near spectral type G. Therefore, within our observing band they would have very different effective wavelengths. In order to check how severe the second-order extinction effect would be, we first determined the effective wavelengths of the L dwarfs and G-type reference stars using the equation

$$\lambda_{\rm eff} = \frac{\int \lambda F_\lambda S_\lambda \, d\lambda}{\int F_\lambda S_\lambda \, d\lambda}, \tag{2}$$

where F_λ is the spectral energy distribution and S_λ is the system response. The L dwarf and reference star spectra were retrieved from digital spectral libraries (Martín et al. 1999; Le Borgne et al. 2003). The computed effective wavelengths for L dwarf and G-type stars are 6308 and 7148 Å, respectively. The average spectroscopic extinctions at IAO are 0.081 and 0.04 mag at these two wavelengths. The difference of these two extinction values is nothing but the second-order extinction correction at the unit air mass, i.e., $k''_R \Delta(R - I)$. The observed color difference $(R - I)$ of L dwarf and G-type reference stars was found to be 2.1 mag, and that predicts $k''_R \approx -0.02$ mag. The second-order extinction coefficient was independently estimated using the observations of the photometric standards and found to be $k''_R \approx -0.02$, similar to the above estimation. The second-order extinction correction was made to each observed L dwarf data using the relation

$$(\Delta m_{i,b})_0 = \Delta m_{i,b} - k''_R \Delta(R - I) X_i, \tag{3}$$

where X_i is the air mass of the frames.

3. RESULTS AND DISCUSSIONS

The light curves of the three L1 dwarfs observed are presented in Figures 1 and 2. Figure 1 shows the light curves of 2MASS 1300+19 and 2MASS 1439+19 in the *R* band, while Figure 2 shows the light curves of 2MASS 1658+70 in both the *R* and *I* bands. The light curves in the *R* band for all three objects indicate a possible variability.

In order to verify any variability, we employ the procedure

TABLE 2

Observing Log and Results

Name	Dates	Frames (Used/Total)	Reference Stars	Filter	$\sigma_{\rm rms}$[a] of L Dwarfs	$\sigma_{\rm rms}$[b] Used in χ^2	p (%)
2MASS 1300+19 ……	2004 Feb 19	13/15	5	*R*	0.019	0.012	>99.0
	2004 May 21	21/24	5	*R*	0.020	0.012	>99.0
2MASS 1439+19 ……	2004 Apr 17	20/24	5	*R*	0.017	0.012	>99.0
	2004 Apr 18	21/24	5	*R*	0.016	0.012	>98.5
2MASS 1658+70 ……	2004 May 19	24/25	5	*R*	0.014	0.018	10.1
	2004 May 20	15/15	5	*R*	0.012	0.018	4.5
	2004 May 21	9/9	5	*R*	0.011	0.018	6.1
	2004 Jun 16	24/24	3	*I*	0.005	0.007	3.1

[a] $\sigma_{\rm rms}$ about the mean differential magnitude of the L dwarf.

[b] $\sigma_{\rm rms}$ used in the χ^2 test, obtained from standard deviation (σ_R) vs. standard *R* magnitude relation.

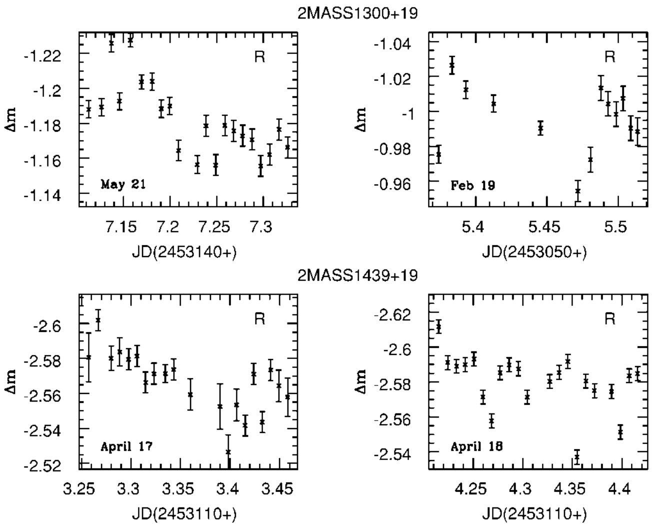

FIG. 1.—*R*-band light curves of the L1 dwarfs 2MASS 1300+19 (*top*) and 2MASS 1439+19 (*bottom*) obtained on different nights.

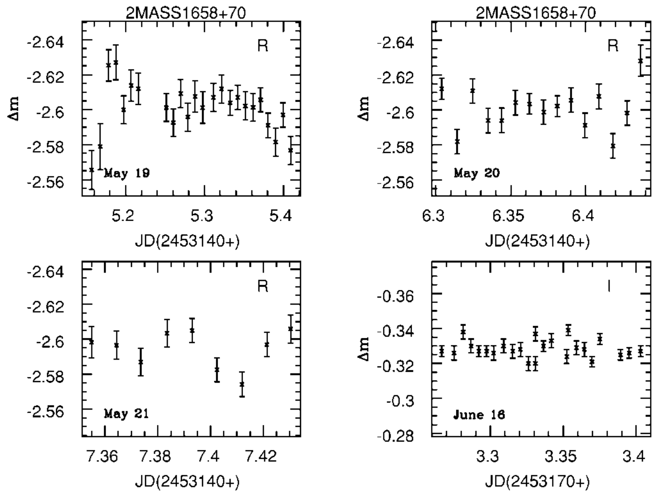

FIG. 2.—*R*- and *I*-band light curves of the L1 dwarf 2MASS 1658+70 obtained on different nights.

given by Martín et al. (2001). In Figures 3*a*–3*e*, we show the standard deviation, σ_R with respect to the standard *R* magnitudes of all the field stars for different fields at different nights along with that for the three targets. Figures 3*a*–3*d* show that although the program stars 2MASS 1300+19 and 2MASS 1439+19 lie at the variable side of the σ_R versus *R* magnitude diagram, no overwhelming evidence for variability in either of the two objects is found. On the other hand, Figure 3*e* shows that the program object 2MASS 1658+70 lies at the nonvariable side of the diagram for May 19, implying no variability in the *R* band. A similar inference can be made from the other observing nights for the *R*-band as well as for the *I*-band observation of the same object.

From Figures 3*a*–3*e*, we notice that for the same field there is much less variation of systematic errors on different nights. Also, for different fields the relation between σ_R with standard *R* magnitudes and its 1 σ scatter do not change significantly. In order to have objects well distributed across the entire magnitude range, we combine the different fields. This should provide a statistically more reliable result for the σ_R versus *R* magnitude relationship. The result with combined fields is presented in Figure 3*f*. For this case, the relation between σ_R and standard *R* magnitudes can be written as

$$\sigma_R = 0.712139 - 0.0854801R + 0.00256972R^2, \qquad (4)$$

with a scatter of 0.004 (1 σ). However, the results do not differ from that obtained by using the individual fields. The objects 2MASS 1300+19 and 2MASS 1439+19 are found to be nearly 2 σ and 1 σ away from the mean relation, respectively.

On the other hand, if we determine the systematic error from the relation between σ_R and standard *R* magnitude and consider its large 1 σ error as well, the systematic error becomes about double the photometric error, which is calculated using ensemble references and program star photometric errors. Even if we add the scatter due to the color effect, such a large error is not expected. However, if we discard the objects that are fairly out of the fit in Figure 3*f* as well as having a systematic trend in their light curve and consider the rest of the field objects instead, the scatter of distribution of error reduces to 0.002 (1 σ). Consequently, the objects 2MASS 1300+19 and 2MASS 1439+19 are found to be situated at about 5 σ and 3 σ away from the mean relation, respectively. Therefore, our analysis implies variability of 2MASS 1300+19 and 2MASS 1439+19 in the *R* band.

The statistical significance of the observed variability is also checked by computing the χ^2 by using the formula

$$\chi^2 = \sum_{i=1}^{n} \left(\frac{\overline{\Delta m_b} - \Delta m_{i,b}}{\sigma_{i,b}} \right)^2 , \qquad (5)$$

where *n* is the number of observed data points and $\sigma_{i,b}$ is the error associated with the L dwarfs at their respective magni-

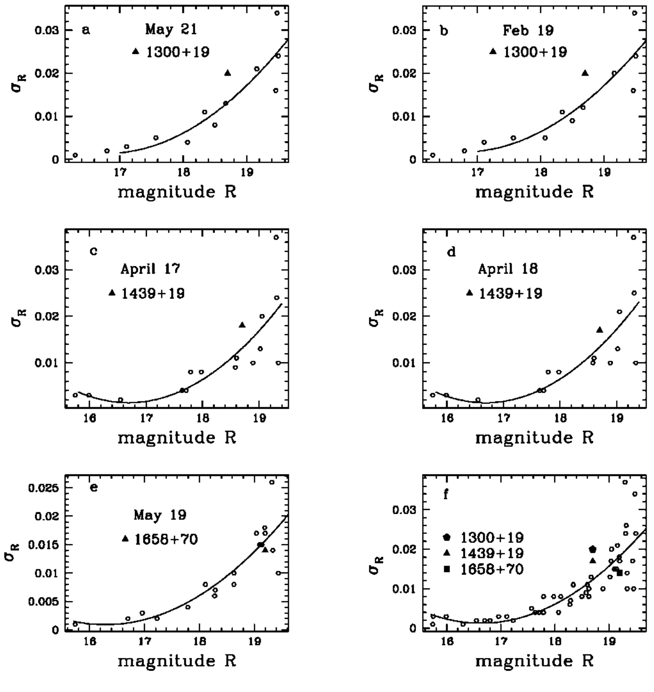

FIG. 3.—Standard deviation (σ_R) vs. *R*-band magnitudes for the field stars for three different fields for individual nights. A second-order polynomial fit to σ_R is shown as a continuous curve. The $\sigma_{\rm rms}$ on each night for all three L1 dwarfs is also shown as filled symbols. The result with combined data of May 21, April 17, and May 19 is given in plot *f*.

tudes, as obtained from the standard deviation versus standard magnitude relation given by equation (4). However, it is worth mentioning that the ratio between the variance of L dwarf data and the variance read from the fitted curve may not have a χ^2 distribution and hence it should be considered as an assumption. Table 2 gives the results for each object for individual nights of observation, the number of good frames taken for final analysis, the number of references taken to make the mean standard, the standard deviation of the points from the mean level ($\sigma_{\rm rms}$), the average $\sigma_{\rm rms}$ used for the χ^2 test, and the probability that the L dwarf is variable (p). The L dwarfs 2MASS 1439+19 and 2MASS 1300+19 indicate variability with about 99% probability for all the observed nights. Note that $\sigma_{i,b}$ are calculated from the σ_R versus R magnitude relation by considering all the field stars including those that show a systematic trend in their light curve.

A period analysis program based on the widely used Scargle formalism (Scargle 1982) was used to search for any periodicity in our time series photometric data. However, we have not obtained any significant periodicity in the variations from either L dwarf.

The third object, 2MASS 1658+70, does not show any variability both in the *R* and the *I* bands. However, while the light curves (see Fig. 2) of May 20 and June 16 look like a scatter plot, there is a systematic trend in the light curves of 2004 May 19 and 21, suggesting a possibility of variation. Furthermore, Gelino et al (2002) reported this object to be variable in the *I* band. It is therefore possible that the variability in this object is transient owing to the dust activity variation. More observations with improved temporal coverage are required to establish the variable nature of 2MASS 1658+70.

4. CONCLUSIONS

R-band differential photometry of three L1 dwarfs—2MASS 1300+19, 2MASS 1439+19, and 2MASS 1658+70—are presented here. The first two objects show variability. However, no periodicity in the variation is obtained in any of these objects. The light curves indicate transient activity of a short timescale. Since rotationally related variability should show rather smooth light curves, any correlation with the rotation of the objects is unlikely. The third object, 2MASS 1658+70, which was also observed in the *I*-band, does not show any variability either in the *R* or in the *I* band, although it was reported to be variable in the *I* band by Gelino et al. (2002). The light curves of this object presented here, however, provide an indication of possible flux variation. More observations of this object are required before its variable nature can be established.

The observation of linear polarization in the red by Menard et al. (2002) favors the presence of a dust cloud in the atmosphere of L dwarfs. The synthetic spectra of L dwarfs also favors the presence of dust in the atmosphere. We propose that the photometric variability in the *R* band reported here arises because of the dust activity in the atmosphere.

On the other hand, if the variability observed is due to the dust activity, then we predict nonzero polarization from L1 dwarfs at the *R* band by dust scattering. However, photospheric variability, if caused by a dust cloud, needs a sufficiently optically thick dust layer. In an optically thick medium, polarization would arise by multiple scattering of photons. It is known that multiple scattering reduces the degree of polarization as compared to that by a single scattering mechanism (Sengupta & Krishan 2001; Sengupta 2003). Hence, a variable L dwarf should show less polarization compared to that of nonvariable or weakly variable objects that might have an optically thin dust layer.

Further observations of L dwarfs of different spectral types and in both the *R* and *I* bands could determine if there is any correlation in the variability at the *R* and *I* bands with the spectral type, which in turn could provide significant insight on the distribution of dust in the atmosphere of L dwarfs.

We are thankful to the referee for many useful suggestions, comments, and constructive criticism. Thanks are due to A. V. Raveendran, A. Saha, and T. P. Prabhu for several discussions.

The observations reported in this Letter were obtained using the 2 m Himalayan Chandra Telescope at Mount Saraswati, Hanle, Indian Astronomical Observatory, the high-altitude station of the Indian Institute of Astrophysics, Bangalore. We thank the staff at IAO and at the remote control station at CREST, Hosakote, for assistance during the observations.

REFERENCES

Bailer-Jones, C. A. L., & Lamm, M. 2003, MNRAS, 339, 477
Bailer-Jones, C. A. L., & Mundt, R. 2001a, A&A, 367, 218
———. 2001b, A&A, 374, 1071
Burrows, A., Hubbard, W. B., Lunine, J. I., & Liebert, J. 2001, Rev. Mod. Phys., 73, 719
Clarke, F. J., Oppenheimer, B. R., & Tinney, C. G. 2002a, MNRAS, 335, 1158
Clarke, F. J., Tinney, C. G., & Covey, K. R. 2002b, MNRAS, 332, 361
Enoch, M. L., Brown, M. E., & Burgasser, A. J. 2003, AJ, 126, 1006
Everett, M. E., & Howell, S. B. 2001, PASP, 113, 1428
Gelino, C. R., Marley, M. S., Holtzman, J. A., Akerman, A. S., & Lodderes, K. 2002, ApJ, 577, 433
Gilliland, R. L., & Brown, T. M. 1988, PASP, 100, 754
Gizis, J. E., et al. 2000, AJ, 120, 1085
Kirkpatrick, J. D., et al. 1999, ApJ, 519, 802
Landolt, A. U. 1992, AJ, 104, 340
Le Borgne, J. F., et al. 2003, A&A, 402, 433
Martín, E. L., Delfosse, X., Basri, G., Goldman, B., Forveille, T., & Zapatero Osorio, M. R. 1999, AJ, 118, 2466
Martín, E. L., Zapatero Osorio, M. R., & Lehto, H. J. 2001, ApJ, 557, 822
Menard, F., Delfosse, X., & Monin, J. 2002, A&A, 396, L35
Scargle, J. D. 1982, ApJ, 263, 835
Sengupta, S. 2003, ApJ, 585, L155
Sengupta, S., & Krishan, V. 2001, ApJ, 561, L123
Sengupta, S., & Kwok, S. 2004, ApJ, submitted
Tsuji, T., Nakajima, T., & Yanagisawa, K. 2004, ApJ, 607, 511
Zapatero Osorio, M. R., Caballero, J. A., Bejar, V. J. S., & Rebolo, R. 2003, A&A, 408, 663